Kinetics of Picosecond Pulse Generation in Semiconductor Lasers with Bimolecular Recombination at High Current Injection

ECKEHARD SCHÖLL, DIETER BIMBERG, HERMANN SCHUMACHER, AND PETER T. LANDSBERG

Abstract—The kinetics of generating ultrashort light pulses by gain switching unbiased semiconductor lasers emitting relaxation oscillations is theoretically modeled and described using phase portraits. Biomolecular recombination processes and realistic injection current pulse shapes are incorporated in the model. Approximate analytical solutions of the rate equations are derived for high current injection. Laser pulse widths, pulse peak power, electrical to optical pulse delay times, and time difference to subsequent relaxation oscillations are computed. Their dependence on injection current to threshold current density ratio (J/J_t) and on material and laser design parameters is explicitly derived and is in good agreement with experiment. In particular the remarkable observation that the laser pulse width is broadly independent of the injection current rise and fall time can thus be understood.

Introduction

In a recent paper [1] the generation of short light pulses by gain switching *unbiased* proton implanted GaAs/GaAlAs double heterostructure semiconductor lasers has been reported. The occurrence of relaxation oscillations is exploited. The pulse width (23 ps FWHM = full width at half-maximum) was found to be largely independent of the rise and fall times of the injection current density J, and is an order of magnitude shorter than these. A new technically simple way, as compared to mode locking for example, for generating probably even shorter pulses has thus been proved to exist. Direct modulation of lasers might become particularly interesting for applications in optical fiber communication close to 1.3 μm, where fiber transmission is high and dispersion is close to zero, such that presence of more than one longitudinal mode does not limit the bit transmission rate.

In this paper, a theory is developed to describe the kinetics of pulse generation for high currents above threshold. Bimolecular recombination processes and realistic injection current pulse shapes are incorporated in the model. Phase portraits are used for the first time here to visualize the solutions of the system of rate equations which describe the kinetics of photons and electrons under time-dependent injection current densities $J(t)$. The phase portraits relate the temporal evolution of the number of charge carriers to the temporal evolution of the number of photons after application of a pulse or a step function until steady state is reached (if ever).

There exist many phenomenological rate equation models using linear [2]-[8] or nonlinear [9]-[17], including bimolecular, recombination rates. Bimolecular band-to-band recombination is known to be dominant in GaAs which is not too strongly doped at room temperature [9]. The theory given below is based on a rate equation model developed recently by two of us under more general aspects [17] and extends it to some specific materials (semiconductors) and excitation conditions of practical importance. In particular the time dependence of the external pumping rate P is taken explicitly into account. Bimolecular band-to-band recombination is used. Consequently the electron life-time is not a constant, but depends on the electron concentration. A merit of our model is that it is simple enough to give clear insight into the mechanism of the kinetics and sophisticated enough to allow for quantitative comparison with and prediction of experimental results.

The Model, Some Numerical Solutions and a Comparison with Experiment

The following processes are taken into account:

i) Stimulated emission and absorption of rate $g\bar{N}$. $\bar{N}$ is the photon density. $g = \tilde{B}(\bar{n} - n_{\mathrm{th}})$ is the gain. $\bar{n}$ is the electron concentration in the n-doped laser active region (N_D completely ionized donors). n_{th} is the electron concentration for which the difference of the electron and hole quasi-Fermi levels equals the bandgap. n_{th} defines the laser threshold for zero photon dissipation κ [17].

ii) Spontaneous emission rate into the lasing mode $B\bar{n}\bar{p}$, where $\bar{p} = \bar{n} - N_D$ is the hole concentration in the laser active region.

iii) Nonradiative transitions and spontaneous emission rate into nonlasing modes $D\bar{n}\bar{p}$.

iv) Photon dissipation rate by cavity loss, scattering etc., $\kappa\bar{N}$.

v) Nonradiative excitation rate by external pumping via a time dependent injection current density $J(t)$.

Manuscript received June 30, 1983; revised October 13, 1983.

E. Schöll was with the Institut für Theoretische Physik, RWTH Aachen, D 5100 West Germany. He is now with the Department of Electrical & Computer Engineering, Wayne State University, Detroit, MI 48202.

D. Bimberg is with the Institut für Festkörperphysik, TU Berlin, D 1000 Berlin 12, West Germany.

H. Schumacher is with the Institut für Halbleitertechnik, RWTH Aachen, D 5100 Aachen, West Germany.

P. T. Landsberg is with the Department of Mathematics, University of Southampton, Southampton, S09 5NH, England.

0018-9197/84/0400-0394$01.00

Other excitation processes like thermal excitation are neglected. $B, \tilde{B}$ and D are transition rate constants ($cm^3 \cdot s^{-1}$), κ^{-1} is the photon lifetime.

The values of the different variables like electron concentration $\bar{n}$, n_{th}, photon density $\bar{N}$, and current density J are replaced by normalized ones:

$$n = \bar{n}/n_t, \quad N = \bar{N}/n_t, \quad n_o = n_{th}/n_t, \quad j = J/J_t,$$

where

$$n_t = n_{th} + \kappa/\tilde{B}, \quad J_t = (B + D)n_t(n_t - N_D) \cdot q \cdot L$$

are the values at the laser threshold, q is the elementary charge and L is the thickness of the laser active layer. The time is scaled in units

$$(\tilde{B}n_t)^{-1} = (1 - n_o)/\kappa,$$

Similarly, dimensionless rate constants $b = BN_D(1 - n_o)/\kappa$, $d = DN_D(1 - n_o)/\kappa$ and a doping parameter $\zeta = n_t/N_D$ are introduced.

Then the following normalized rate equations for the variation of the photon and the electron density are obtained

$$\dot{N} = (n - 1)N + b(\zeta n^2 - n) \tag{1a}$$

$$\dot{n} = (b + d)[(\zeta - 1)j(t) - \zeta n^2 + n] - (n - n_o)N. \tag{1b}$$

Numerical solutions of (1) are shown in Fig. 1 for two different injection currents and two different sets of material parameters. The dimensionless material parameters b, d, n_o, ζ are derived from

$$D = 1.5 \times 10^{-10}\ cm^3\ s^{-1}\ [18], \quad B/D = 10^{-3}\ [3],$$

$$n_{th} = 1.3 \times 10^{18}\ cm^{-3}\ [13], \quad n_t = 6.5 \times 10^{18}\ cm^{-3},$$

$$N_D = 6.5 \times 10^{17}\ cm^{-3},$$

$\kappa^{-1} = 1.25$ ps for Fig. 1(a), (b)

$$(d = 10^{-4}, b = 10^{-7}, n_o = 0.2, \zeta = 10)$$

and

$$n_t = 2.6 \times 10^{18}\ cm^{-3}, \quad N_D = 2.0 \times 10^{17}\ cm^{-3},$$

$\kappa^{-1} = 0.2$ ps [10] for Fig. 1(c)

$$(d = 3 \times 10^{-6}, b = 3 \times 10^{-9}, n_o = 0.5, \zeta = 13).$$

These are typical values for GaAs double heterostructure lasers.

The phase portraits of Fig. 1(a)-(c) show the flow $n(t), N(t)$ of electrons and photons starting at time $t = o$ from the phase point $(n = \zeta^{-1}, N = o)$. This point corresponds approximately to thermal equilibrium, where the electron density is equal to the doping concentration, and the photon density is negligible.

Fig. 1(a) represents the case of a step function injection current density. The time lag between the delayed response of the photon density and the instant increase of electron density is clearly shown. The relaxation oscillations and the decrease of their amplitude with increasing time towards a steady state value of the whole system can be clearly seen. It should be noted that the current density chosen for this phase portrait is 8.6 times the threshold current. The highest value the electron density reaches ($\cong 1.2\ n_t$) is much below that ratio.

Fig. 1(b) in contrast represents the nonstationary case of an

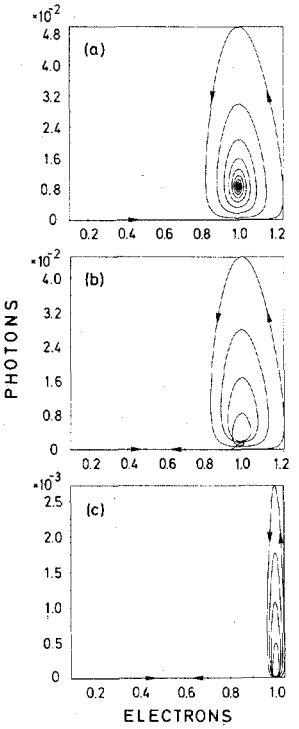

Fig. 1. Phase portraits of photons and electrons with (a) step function injection current $j = 8.6$. (b), (c) j = Gaussian with $j_o = 8.6$, $t_o = 500$ ps, $t_r = 250$ ps, $t_f = 280$ ps. The material parameters are $D = 1.5 \times 10^{-10}\ cm^3 \cdot s^{-1}$, $B/D = 10^{-3}$, $n_{th} = 1.3 \times 10^{18}\ cm^{-3}$ and (a), (b) $n_t = 6.5 \times 10^{18}\ cm^{-3}$, $N_D = 6.5 \times 10^{17}\ cm^{-3}$, $\kappa^{-1} = 1.25$ ps (c) $n_t = 2.6 \times 10^{18}\ cm^{-3}$, $N_D = 2.0 \times 10^{17}\ cm^{-3}$, $\kappa^{-1} = 0.2$ ps. The trajectory corresponding to the initial thermal equilibrium $N = 0$, $n = \zeta^{-1}$ is shown.

injection current pulse. A two-sided Gaussian is chosen, to allow for rise and decay times t_r and t_f, respectively, independent of each other. The normalized current density is

$$j(t) = \begin{cases} j_o \exp - [(t - t_o)/t_r]^2 & \text{for } t < t_o \\ j_o \exp - [(t - t_o)/t_f]^2 & \text{for } t > t_o \end{cases} \tag{2}$$

approximating well the experimentally used current shape. The same $j_o = 8.6$ as in Fig. 1(a), $t_r = 250$ ps and $t_f = 280$ ps are used. The phase portrait shows that fewer relaxation oscillations occur, decaying faster in amplitude. Finally the system is drawn back in the phase plane from $N \cong 0$, $n \cong 1$ to the initial point $N = 0$, $n = \zeta^{-1}$ along the n-axis. This corresponds to the decay of the electrons to thermal equilibrium on the slow time scale d^{-1} by (1b). During the first relaxation oscillation the current $j(t)$ can safely be approximated by its maximum value j_o. In order to obtain a pronounced first relaxation oscillation the time when the peak injection current occurs should roughly be equal to the delay time.

Already at first glance a comparison of the first relaxation oscillation of Fig. 1(a) to the first relaxation oscillation of Fig. 1(b) discloses a great similarity. Indeed numerical calculations with a large number of different injection current pulse shapes show that the shape of the laser pulses is largely independent of rise and fall times of the current. However, a strong dependence on the peak current and some of the intrinsic laser parameters is found. Fig. 1(c) represents a phase portrait with the same injection current as in Fig. 1(b), but with different material

parameters. The donor concentration and the photon lifetime are chosen to be smaller in Fig. 1(c). These values are representative for the lasers used in our experiments. Since n_t and N_D were given by the manufacturer up to an order of magnitude only [19], we determined their exact values by fitting them such that the smallest value j_o for which a laser pulse occurred agreed with the experimental value of $j_o = 6.7$. Note that n_t does not appear explicitly in our calculations as it only scales the occurring concentrations.

Fig. 2 shows the normalized photon density of the laser pulses (relaxation oscillations) versus time for various peak currents j_o and fall times t_f, and the same material parameters as Fig. 1(c).

For a sufficiently slow current fall time t_f and sufficiently large j_o successive relaxation oscillations can also be produced [Fig. 2(b)-(d)]. During each of these, the current can again be approximated by an appropriate constant value $j < j_o$. Hence, the successive, if any oscillations are centered around phase points to be labeled (n^*, N^*). Successively smaller N^* are found according to (3) below. The peaks of these successive oscillations are the more pronounced the larger j_o, and the slower the current fall time t_f is. They are completely suppressed for short t_f [Fig. 2(a)] or small j_o [Fig. 2(e)]. This is shown in Fig. 2(a)-(c) where t_f increases from 150-280 ps and in Fig. 2(c)-(e) where j_o decreases from 8.6-6.7. The peak height of the oscillations falls faster than normal relaxation oscillations at constant $j = j_o$ would, and the FWHM of each of them becomes successively broader.

With increasing j_o the full width at half maximum (t_{FWHM}) of the first relaxation oscillation, the distance between subsequent oscillations T and the delay time τ_d between current and photon pulse decrease, the peak power (proportional to the peak photon density $N_{\max}$) of the laser pulses on the other hand increases dramatically. Fig. 3(a)-(d) show explicitly the dependence of these four quantities on injection current density for a larger current range.

The independence of the shape of the first relaxation oscillation of the injection current pulse shape is in good agreement with the experimental findings of Klein *et al.* [1].

In order to compare with the theoretical predictions for the j-dependence of t_{FWHM}, τ_d, T, and $N_{\max}$ we made a number of new experiments using the experimental set-up described in [1]. The transient photocurrent from a Schottky-diode was displayed on a fast sampling-oscilloscope ($t_r \cong 20$ ps). The overall response of the detection system was determined to have a FWHM of about 28 ps by means of a 2 ps pulse from a mode-locked dye laser. Since the measured signal (Fig. 4) is the convolution of the photon pulse $N(t)$ with the response of the detection system, the pulse widths are significantly broadened. The results for τ_d and T are included in Fig. 3. Excellent agreement with theory is found. Due to lack of time resolution unfortunately no similar comparison can be yet made for FWHM and peak power, which are certainly the more important quantities from the point of view of applications. From the theoretical analysis it seems to be feasible to produce laser pulses narrower than 10 ps, having a peak power far beyond 1 W.

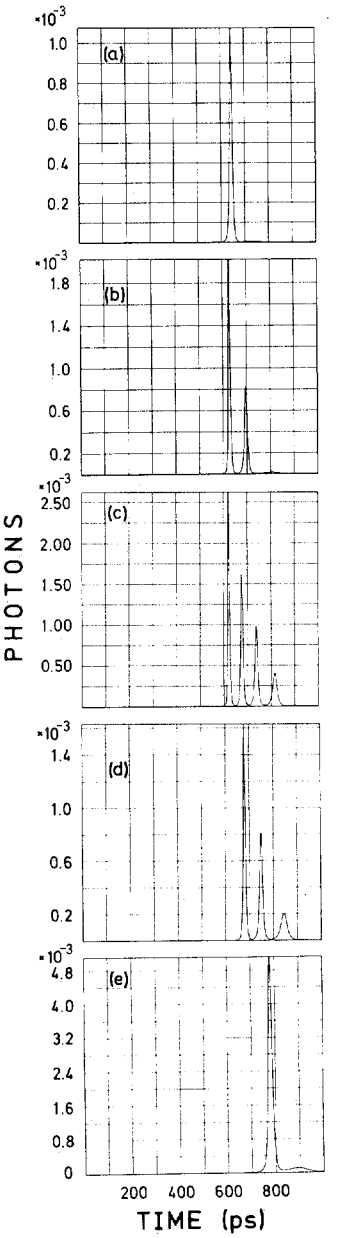

Fig. 2. Photon concentration in units of n_t versus time as numerical solution of the rate equations (1) with the same material parameters as in Fig. 1(c). The injection current in modeled Gaussian according to (2) with $t_o = 500$ ps, $t_r = 250$ ps.

(a) $t_f = 150$ ps, $j_o = 8.6$

(b) $t_f = 200$ ps, $j_o = 8.6$

(c) $t_f = 280$ ps, $j_o = 8.6$

(d) $t_f = 280$ ps, $j_o = 7.6$

(e) $t_f = 280$ ps, $j_o = 6.7$

Analytical Solutions

In order to gain deeper physical insight into the mechanism of the laser pulse generation, we shall try to obtain analytical expressions for the delay time and the width of the laser pulse. First, solutions of (1) in terms of phase portraits for the flow $n(t)$ and $N(t)$ (Fig. 1) are discussed in more detail.

Neglecting spontaneous emission into the lasing mode ($b = 0$),

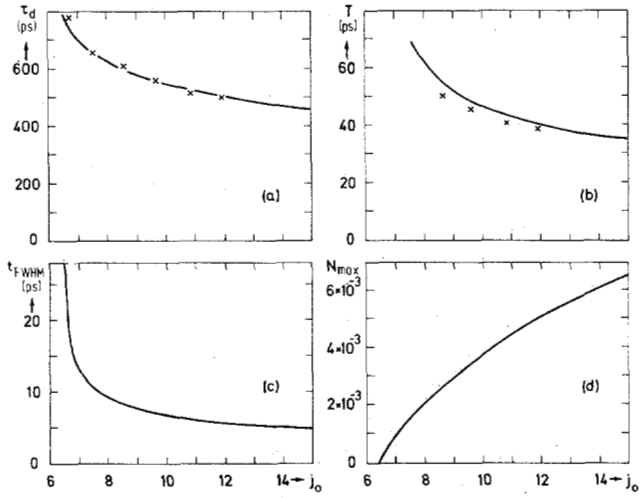

Fig. 3. Delay time τ_d, width of the photon pulse t_{FWHM}, spacing of the first two relaxation oscillations T, and amplitude of the first relaxation oscillation N_{max} (= peak power in arbitrary units) as a function of j_o. The crosses are experimental values, the lines are numerically calculated [parameters as in Fig. 1(c)].

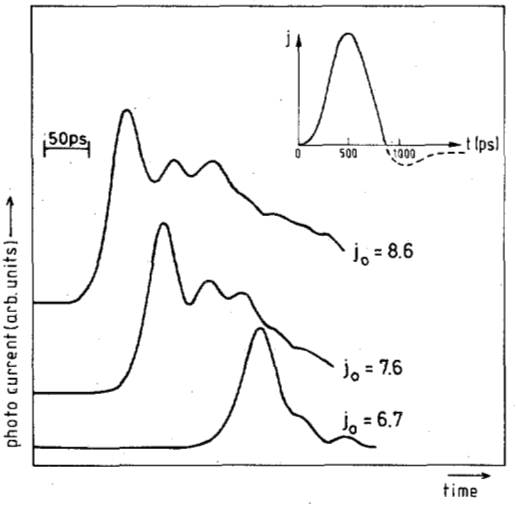

Fig. 4. Measured response of a GaAs Schottky diode to three laser pulses with different injection currents corresponding to Fig. 2(c)–(e). The insert shows the applied injection current pulse shape versus time (FWHM: 440 ps).

the steady state (n^*, N^*) of (1) for a constant current is given by

$$N^* = 0,\ n^* = (1 + \sqrt{1 + 4\zeta(\zeta - 1)j})/(2\zeta)$$

$$\text{for } j < 1 \text{ (below threshold)}$$

$$N^* = d\,\frac{\zeta - 1}{1 - n}\,(j - 1), \qquad n^* = 1$$

$$\text{for } j > 1 \text{ (above threshold)} \tag{3}$$

For fixed j, the flow of photons $N(t)$ and of electrons $n(t)$ is always directed towards the appropriate steady state, which is therefore always stable.

The steady state is defined by the intersection of the curves $\dot{N} = 0$ and $\dot{n} = 0$, which are respectively

$$N = 0,\ n = 1 \tag{4a}$$

and

$$N = d[(\zeta - 1)j - \zeta n^2 + n]/(n - n_o). \tag{4b}$$

The question of the path in the (n, N)-plane by which the steady state (n^*, N^*) is approached can be answered by linearizing (1) around this steady state and solving the rate equations explicitly in its neighborhood. If the discriminant

$$\Delta = d\{(\zeta - 1)(j - 1) - \tfrac{1}{4}d[2\zeta - 1 + (\zeta - 1)(j - 1)/(1 - n_o)]^2\} \tag{4c}$$

is positive, all trajectories spiral around a "focus" (n^*, N^*) with angular frequency $\omega = \sqrt{\Delta}$. If $\Delta < 0$, the steady state represents a "node," i.e., any trajectory approaches the steady state along one of two straight lines in the phase plane with different but fixed slope dN/dn. In our model $\Delta = 0$ singles out an injection current density $j_1 \gtrsim 1$ below which the steady state is a node and above which it is a focus. For physically reasonable parameters $(d << 1)$ we find approximately $j_1 \cong 1$.

For a time-dependent j the curve $\dot{n} = 0$ (4b) changes, and with it the whole flow picture of the phase portrait. Hence, in contrast to the standard phase portraits for autonomous systems of differential equations, a trajectory $(n(t), N(t))$ can intersect itself as shown in Fig. 1(b).

Initially, at $t = 0$ we have $j = 0$, and hence, by (3) the steady state is $N^* = 0$, $n^* = \zeta^{-1}$. As j increases, the steady state first moves along the n-axis, and then, above threshold, along the line $n = 1$, by (3). The flow is directed away from the initial point $N^* = 0$, $n^* = \zeta^{-1}$, as indicated in Fig. 1. The increase of photons by (1a) is negligible as long as $n < 1$, and the electron number $n(t)$ increases by (1b) with $N \cong 0$. If the current density $j(t)$ rises sufficiently fast on the time scale of the electronic transitions (d^{-1}), the phase point $(n(t), N(t))$ remains at sufficient distance from the actual steady state (n^*, N^*) in the phase plane, i.e., $(\zeta - 1)j(t) >> \zeta n(t)^2 - n(t)$. Hence, the recombination term in (1b) may be neglected, and $n(t)$ is given approximately by

$$n(t) = \zeta^{-1} + d(\zeta - 1)j_o \int_o^t f(t')\,dt' \tag{5}$$

where $f(t)$ is the current shape function.

The delay time τ_d for the onset of the photon pulse can be defined by $n(\tau_d) = 1$. Experimentally, it may be more appropriate to define τ_d by building up a certain minimum photon concentration, but this only shifts τ_d by a small quantity. For a square-shaped injection current it follows from (5)

$$\tau_d^{square} \cong [1 - \zeta^{-1}]\,[d(\zeta - 1)j_o]^{-1} = (d\zeta j_o)^{-1}. \tag{6a}$$

In dimensional time units the delay time is $(Dn_t j_o)^{-1}$. For an exponentially rising injection pulse $(f(t) = 1 - \exp(-t/t_r))$ one finds for $t_r << \tau_d$:

$$\tau_d \cong \tau_d^{square} + t_r. \tag{6b}$$

For a Gaussian pulse $f(t) = \exp - [(t - t_o)/t_r]^2$ with $t_r << t_o \lesssim \tau_d$ one has

$$\tau_d \cong \tau_d^{square} + t_o - \frac{\sqrt{\pi}}{2}\,t_r. \tag{6c}$$

Quite generally the approximations [(6a)-(6c)] are valid for large j_o as used in our experiments. Due to the neglect of recombination the approximate delay times are slightly too small. For the parameters appropriate to our experiments [see caption of Fig. 1(c)] the error as compared to the numerical solution [Fig. 3(a)] is 8 percent for $j_o = 7$, 5 percent for $j_o = 7.6$ and below 2 percent for $j_o \geqq 10$. Note that in case of step-currents more sophisticated expressions for τ_d are available [9], [11].

For $n > 1$ stimulated emission becomes effective, and the photon number increases. Relaxation oscillations are initiated. During each of these the current $j(t)$ may be approximated by an appropriate constant value j. From (1), linearized around the steady state (n^*, N^*) for fixed $j \cong j_o$, one finds oscillatory solutions $\delta N(t)$, $\delta n(t) \sim e^{-\lambda t} e^{-i\omega t}$ ($\delta N := N - N^*$), $\delta n := n - n^*$) with damping constant

$$\lambda = d[2\zeta - 1 + (\zeta - 1)(j_o - 1)(1 - n_o)^{-1}]/2 \tag{7}$$

and period

$$T := 2\pi/\omega \cong 2\pi/\sqrt{d(\zeta - 1)(j_o - 1)} \quad \text{for} \quad d \ll 1. \tag{8}$$

In the linear approximation the first relaxation oscillation for $\lambda \ll \omega$ is almost an ellipse centered around the steady state $N^* = d(\zeta - 1)(j - 1)/(1 - n_o)$, $n^* = 1$ with maximum photon concentration $2N^*$. Hence, in the linear approximation the FWHM of the photon pulse is $T/2$, i.e., in dimensional time units $\pi\{(n_t - n_{th})/[(n_t - N_D)Dn_t\kappa(j_o - 1)]\}^{1/2}$. However, from the phase portrait [Fig. 1(a)] it is obvious that the peak photon concentration N_{max} is drastically increased by the nonlinearities in (1), such that the FWHM becomes essentially shorter than $T/2$. This effect is the stronger, the larger j_o is.

An approximation of the nonlinear FWHM can be computed by retaining, in the photon rate equation, in addition to the terms arising from the linearization around (n^*, N^*), the full nonlinear gain and loss terms. An exact first integral of the rate equations can then be obtained [20]. If the second integration is carried out approximately up to lowest order in the small parameter $N^*/\delta N$, the following FWHM is found:

$$t_{FWHM} \cong 0.8\sqrt{N^*/(N_{max} - N^*)}\, T/2. \tag{9}$$

For Fig. 2(c), e.g., this means $t_{FWHM} \cong 0.4 \cdot T/2$.

Obviously this approximation is good if $N^*/(N_{max} - N^*)$ is small, i.e., for a large overshoot of N_{max} over N^*, as is the case for large j_o. For the parameters appropriate to our experiments there is excellent agreement with the numerical result, the error being less than 6 percent for $j_o \geqq 7.6$ in Fig. 3(c).

Alternative approximations of t_{FWHM} were given by Van der Ziel and Logan [21] for combined dc and microwave current injection. Their analytical approximations are valid for dc currents close to threshold and are thus complementary to our calculations.

Conclusion

In conclusion, the kinetics of extremely short laser pulses and the dependence of their delay time, their width, the number and spacing of successive relaxation oscillations and the peak photon concentration upon the injection current $j(t)$ and the electron and photon lifetimes can be readily understood from the above phase portrait analysis which used a novel technique for explicitly time-dependent rate systems. It is evident that the laser pulse width is not sensitive to a variation of the rise and fall times of the injection current as long as the rise time is smaller than the delay time of the laser pulse. Analytical approximations of the delay time and the FWHM have been obtained in the case of high peak injection currents well above threshold ($J/J_t > 7$). Our analysis suggests that the FWHM decreases approximately as the inverse square root of the peak injection current (in excess of the threshold current).

We have also used other sets of material parameters in order to check the sensitivity of our numerical results to these values. For instance, we have varied the donor concentration in the range $N_D = 4 \times 10^{16} \cdots 1 \times 10^{18}$ cm^{-3}, which produced only slight changes in the pulse width ($t_{FWHM} = 6.5 \cdots 8.5$ ps for $j_o = 10$). An increase of the spontaneous emission coefficient B/D by a factor of 10 increases the FWHM by one third and decreases N_{max} by one third for $j_o = 10$. Further increase of B/D eventually suppresses the relaxation oscillations altogether—an effect which has already been pointed out previously [3]. A decrease of D or κ increases all relevant times significantly (τ_d, T, t_{FWHM}). However, our experimental findings for τ_d and T as well as other references [10], [18] strongly support our choice of values for D and κ. Thus within reasonable ranges of material parameters our numerical and analytical results suggest the feasability of even shorter pulses than previously obtained down to the 10 ps range. Experimental work on this has started, but no results can be presented as yet.

The inclusion of the bimolecular recombination term is essential for the modeling of the experiments considered. The photon pulse depends sensitively upon this nonlinearity in the rate equations, because the electron lifetime changes considerably during the transient process. The effective electron lifetime τ_e defined by linear regression to the steady state $n^*(\delta\dot{n} = -\delta n/\tau_e)$ is given by $\tau_e = d^{-1}[2\zeta n^* - 1]^{-1}$. This yields $\tau_e = d^{-1}$ at thermal equilibrium, but $\tau_e = d^{-1}(2n_t/N_D - 1)^{-1}$ at threshold, which differs, for example, by a factor of 25 for the parameters of Figs. 2. Thus, it is impossible to model the whole transient process by a single constant lifetime.

Acknowledgment

We are grateful to Dr. M. Osinski, Southampton, England, for discussion.

References

[1] H. J. Klein, D. Bimberg, H. Beneking, J. Kuhl, and E. O. Göbel, "High peak power picosecond light pulses from a directly modulated semiconductor laser," *Appl. Phys. Lett.*, vol. 41, pp. 394–396, 1982.

[2] R. Salathé, C. Voumard, and H. Weber, "Rate equation approach for diode lasers," *Opto-Electronics*, vol. 6, pp. 451–456. 1974.

[3] P. M. Boers, M. T. Vlaardingerbroek, and M. Danielsen, "Dynamic behaviour of semiconductor lasers," *Electron. Lett.*, vol. 11, pp. 206–208, May 1975.

[4] D. J. Channin, "Effect of gain saturation on injection laser switching," *J. Appl. Phys.*, vol. 50, pp. 3858–3860, June 1979.

[5] J. P. Van der Ziel, J. L. Merz, and T. L. Paoli, "Study of intensity pulsations in proton-bombarded stripe-geometry double-heterostructure $Al_xGa_{1-x}As$ lasers," *J. Appl. Phys.*, vol. 50, pp. 4620–4637, July 1979.

[6] J. M. Vilela, F. D. Nunes and N. B. Patel, "Transient effects in single heterostructure GaAs lasers," *IEEE J. Quantum Electron.*, vol. QE-15, pp. 801–806, Aug. 1979.

[7] R. W. Dixon and W. B. Joyce, "A possible model for sustained oscillations (pulsations) in (Al,Ga)As double-heterostructure lasers," *IEEE J. Quantum Electron.*, vol. QE-15, pp. 470–474, June 1979.
[8] H. Ito, H. Yokoyama, S. Murata, and H. Inaba, "Generation of picosecond optical pulses with highly RF modulated AlGaAs DH lasers," *IEEE J. Quantum Electron.*, vol. QE-17, pp. 663–670, May 1981.
[9] G. W. 't Hooft, "The radiative recombination coefficient of GaAs from laser delay measurements and effective nonradiative carrier lifetimes," *Appl. Phys. Lett.*, vol. 39, pp. 389–390, Sept. 1981.
[10] T. L. Paoli, "Magnitude of the intrinsic resonant frequency in a semiconductor laser," *Appl. Phys. Lett.*, vol. 39, pp. 522–524, Oct. 1981.
[11] R. W. Dixon and W. B. Joyce, "Generalized expressions for the turn-on delay in semiconductor lasers," *J. Appl. Phys.*, vol. 50, pp. 4591–4595, July 1979.
[12] J. P. van der Ziel, "Time-dependent voltage measurements of pulsating $Al_xGa_{1-x}As$ double-heterostructure lasers," *Appl. Phys. Lett.*, vol. 35, pp. 116–118, July 1979.
[13] K. D. Chik, J. C. Dyment, and B. A. Richardson, "Self-sustained pulsations in semiconductor lasers: Experimental results and theoretical confirmation," *J. Appl. Phys.*, vol. 51, pp. 4029–4037, Aug. 1980.
[14] B. S. Poh and T. E. Rozzi, "Intrinsic instabilities in narrow stripe geometry lasers caused by lateral current spreading," *IEEE J. Quantum Electron.*, vol. QE-17, pp. 723–731, May 1981.
[15] T. Mukai and Y. Yamamoto, "Gain, frequency bandwidth and saturation output power of AlGaAs DH laser amplifiers," *IEEE J. Quantum Electron.*, vol. QE-17, pp. 1028–1034, June 1981.
[16] M. J. Adams and M. Osinski, "Longitudinal mode competition in semiconductor lasers," *Proc. IEE*, vol. 129, pp. 271–274, Dec. 1982.
[17] E. Schöll and P. T. Landsberg, "Non-equilibrium kinetics of coupled photons and electrons in two-level systems of the laser type," *J. Opt. Soc. Am.*, vol. 9, pp. 1197–1206, Sept. 1983.
[18] C. J. Hwang and J. C. Dyment, "Dependence of threshold and electron lifetime on acceptor concentration in GaAs-$Ga_{1-x}Al_xAs$ lasers," *J. Appl. Phys.*, vol. 44, pp. 3240–3244, July 1973.
[19] H. P. Vollmer, AEG-Telefunken KE2-ULM, private communication.
[20] E. Schöll, to be published.
[21] J. P. van der Ziel and R. A. Logan, "Generation of short optical pulses in semiconductor lasers by combined dc and microwave current injection," *IEEE J. Quantum Electron.*, vol. QE-18, pp. 1340–1350, Sept. 1982.

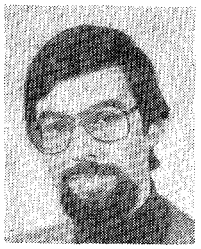

Eckehard Schöll was born in Stuttgart, West Germany, on February 6, 1951. He received the Diplom degree in physics from the University of Tübingen, West Germany, in 1976. Afterwards, he held an overseas followship from the German National Scholarship Foundation, which he spent at the Department of Mathematics, University of Southampton, England, where he received the Ph.D. degree in 1978.

Since 1978, he has been with the Institute of Theoretical Physics at the Rheinisch-Westfälische Technische Hochschule Aachen, West Germany, where he received the Dr.rer.nat. degree (summa cum laude) in 1981. He is currently spending a sabbatical year with the Department of Electrical and Computer Engineering, Wayne State University, Detroit, MI, investigating nonlinear transport and current instabilities in semiconductors. His research interests include instabilities and nonequilibrium phenomena in semiconducotors, in particular, impact ionization induced current filamentation and threshold switching, nonequilibrium phase transitions, nonlinear optical and hot electron effects, nonlinear semiconductor laser kinetics.

Dr. Schöll received the Borchers Medal from the Rheinisch-Westfälische Technische Hochschule Aachen in 1983. He is a member of the German Physical Society (DPG).

Dieter Bimberg, photograph and biography not available at the time of publication.

Hermann Schumacher, photograph and biography not available at the time of publication.

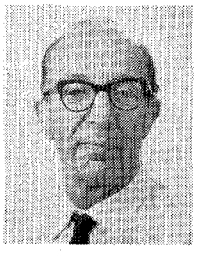

Peter T. Landsberg received the D.Sc. degree from the University of London, London, England

He has been Dean of the Mathematics Faculty in Southampton and previously in Cardiff, where he was also Deputy Principal for some years. He has served on the Councils of both The Institute of Mathematics and its Applications. He is currently also a Visiting Professor at the University of Florida, Gainesville, FL. He is the author of many research papers and several books in areas ranging from solar cells to thermodynamics and relativity. He has broadcast on radio and television in the UK and USA and has lectured throughout the world—he was the Saha Memorial Lecturer in Calcutta (1979). He has also been active as an organizer of international conferences on thermodynamics (1970), semiconductors (1978), and solar cells (1982).